Quantum Electronics **44** (11) 993–996 (2014)

PACS numbers: 42.55.Px; 42.60.Jf; 42.60.Lh; 85.35.Be
DOI: 10.1070/QE2014v044n11ABEH015563

Saturation of light–current characteristics of high-power lasers (λ = 1.0–1.1 μm) in pulsed regime

D.A. Veselov, V.A. Kapitonov, N.A. Pikhtin, A.V. Lyutetskiy, D.N. Nikolaev, S.O. Slipchenko, Z.N. Sokolova, V.V. Shamakhov, I.S. Shashkin, I.S. Tarasov

Abstract. **Semiconductor lasers based on MOVPE-grown asymmetric separate-confinement heterostructures with a broadened waveguide and emitting in the wavelength range 1.0–1.1 μm are studied. It is found that the intensity of spontaneous emission from the active region increases with increasing pump current above the lasing threshold and that this is caused by a growth in the concentration of charge carriers in the active region due to the modal gain enhancement needed to compensate for the growing internal optical loss at high pulsed pump currents. It is shown that the increase in the internal optical loss with increasing pulsed pump current is one of the main reasons for saturation of the light–current characteristics of high-power semiconductor lasers.**

Keywords: *semiconductor laser, internal optical loss, pulsed pumping, spontaneous emission.*

1. Introduction

Semiconductor lasers emitting in the wavelength range 1000–1100 nm are used both as individual radiation sources and for optical pumping [1]. With improvement of the output power characteristics of these lasers, they become a more and more attractive alternative to lasers of other types. Continuous-wave semiconductor lasers operating in this wavelength region have already demonstrated close-to-limiting radiation characteristics [2–4]. However, in the case of pumping by high-current pulses with durations of several hundreds of nanoseconds, the light–current characteristics of theses lasers saturate independently of the growth technology and the composition of the used semiconductor solid solutions [2, 3, 5]. The reasons for the saturation of pulsed power at high pump currents were studied in a number of works, which considered the factors responsible for this saturation. Among these factors are the growth of the concentration of charge carriers in the waveguiding layers, electron leakage current in the waveguide and p-emitter, lasing of highest transverse modes, gain saturation and ‘burning’ of charge carriers [2–8], as well as non-instantaneous capture of carriers into the quantum-well active region [9].

In the present work, we continue experimental and theoretical investigations in order to determine the possible reasons for the saturation of the optical power of pulsed semiconductor lasers based on the AlGaAs/InGaAs/GaAs solid solution system at high pump currents.

2. Experimental samples and main methods

We studied semiconductor lasers based on an asymmetric separate-confinement quantum-well heterostructure with a broadened waveguide grown by the MOVPE method [10]. At present, this laser structure is standard and commonly used in cw semiconductor lasers, but it is not optimised for operating in pulsed regime. The laser heterostructure parameters are listed in Table 1. The composition of the waveguide solid solution is chosen taking into account the necessity of suppression of charge delocalisation from the active region into the waveguiding layers [11, 12]. The waveguide width is increased to decrease the internal optical loss, the beam divergence, and the optical power density at the output mirror of the laser [13, 14]. The composition of the laser heterostructure emitters was calculated so that the optical confinement factor was minimal in the emitter layers and maximal in the active region [13, 14]. The active region consists of two quantum wells, whose thickness ensures the existence of one electronic transition in the spontaneous and stimulated emission spectra.

Table 1. Laser heterostructure parameters.

Layer	Thickness	Composition	Doping/cm^{-3}
barrier	0.45 μm	GaAs	$n = 5 \times 10^{18}$
n-emitter	2 μm	$Al_{0.3}Ga_{0.7}As$	$n = 5 \times 10^{18}$
n-waveguide	1.64 μm	$Al_{0.1}Ga_{0.9}As$	undoped
quantum well	63 Å	$In_xGa_{1-x}As$	undoped
barrier	200 Å	$Al_{0.1}Ga_{0.9}As$	undoped
quantum well	63 Å	$In_xGa_{1-x}As$	undoped
p-waveguide	1.16 μm	$Al_{0.1}Ga_{0.9}As$	undoped
p-emitter	1.2 μm	$Al_{0.6}Ga_{0.4}As$	$p = 5 \times 10^{18}$
contact	0.3 μm	GaAs	$p = 5.4 \times 10^{19}$

Single semiconductor lasers with a 100-μm lasing aperture were made using constructions with deep mesas, when the active layer lies between deep steep mesas etched through the whole laser structure, which helps to avoid quenching of lasing [15, 16]. The studied emitters had different lengths of the Fabry–Perot cavities and were mounted on a copper heat sink with the mesa structures face down. In contrast to our previous works [11, 17], to observe spontaneous emission in

D.A. Veselov, V.A. Kapitonov, N.A. Pikhtin, A.V. Lyutetskiy, D.N. Nikolaev, S.O. Slipchenko, Z.N. Sokolova, V.V. Shamakhov, I.S. Shashkin, I.S. Tarasov Ioffe Institute, Russian Academy of Sciences, ul. Politekhnicheskaya 26, 194021 St. Petersburg, Russia; e-mail: nike@hpld.ioffe.ru

Received 22 May 2014; revision received 3 July 2014
Kvantovaya Elektronika **44** (11) 993–996 (2014)
Translated by M.N. Basieva

the samples in the present work, we formed a window in the upper ohmic contact layer from the side of the substrate (Fig. 1). The window was 100 × 50 μm in size, owing to which the part of spontaneous emission coupled out of the window was constant in the entire range of pump currents. This geometry of the experiment makes it possible to decrease the fraction of stimulated emission when recording the spontaneous component of emission from the active region of the laser structure.

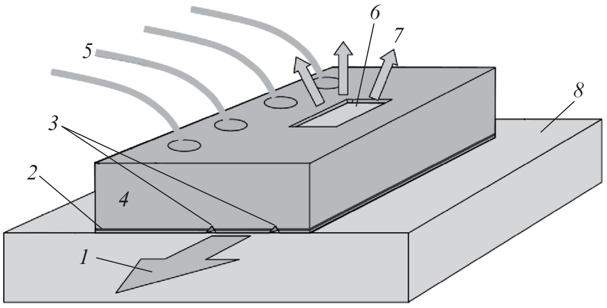

Figure 1. Schematic of the sample for investigation of spontaneous emission through the substrate: (*1*) stimulated laser emission; (*2*) laser heterostructure; (*3*) mesastrips; (*4*) GaAs substrate; (*5*) gold wires; (*6*) window in the n-contact; (*7*) spontaneous emission passed through the substrate; (*8*) heat sink.

To study the electroluminescent characteristics of semiconductor lasers, we used a current pulse generator, which formed pulses with an amplitude up to 100 A, a duration at half maximum of 100 ± 20 ns, and a repetition rate of 1040 ± 20 Hz. The current was controlled by the voltage on a 0.2-Ohm resistor connected in series with the laser. The voltage was recorded by a Tektronix TDS2024C oscilloscope.

The light–current characteristics of all the samples were measured in two steps: first, we measured the average power by a 3A-P-FS-12 (Ophir Photonics) bolometer and then determined the light pulse shape using an IS200-4 integrating sphere and a SM05PD4A photodetector (both from Thorlabs). Based on these data, we calculated the maximum optical power of the laser.

3. Study of spontaneous laser emission in pulsed regime

The saturation of the light–current characteristics of semiconductor lasers can be caused by two reasons, namely, by a decrease in the internal quantum efficiency of stimulated emission $\eta_{\rm in}$ and by an increase in the internal optical loss $\alpha_{\rm in}$. The decrease in the $\eta_{\rm in}$ coefficient corresponds to a current leakage above the lasing threshold due to, for example, recombination in the waveguide or to a leakage of electrons to the p-emitter. In this case, the radiative characteristics of the active region do not change (excluding the changes caused by possible heating). The second reason – increase in the internal optical loss $\alpha_{\rm in}$ – leads to a decrease in the slope of the light–current characteristic, which is illustrated by the well-known dependence of the output power P on the pump current I

$$P = \eta_{\rm in} \frac{\alpha_{\rm out}}{\alpha_{\rm out} + \alpha_{\rm in}} \frac{h\nu}{q} (I - I_{\rm th}). \tag{1}$$

Here, $\alpha_{\rm out}$ is the optical output mirror loss, $h\nu$ is the photon energy, q is the electron charge, and $I_{\rm th}$ is the threshold current or the current needed to compensate for all losses. Assuming that the internal optical loss $\alpha_{\rm in}$ increases with the pump current, the threshold current $I_{\rm th}$ can be represented in the form $I_{\rm th} = I^*_{\rm th} + \Delta I^*_{\rm th}$, where $I^*_{\rm th}$ is the threshold current consisting of the current spent on the spontaneous luminescence and the nonradiative recombination, and $\Delta I^*_{\rm th}$ is the increase in the $I^*_{\rm th}$ current needed to increase the modal gain and compensate for the internal optical losses increased with increasing pump current. The intensity of spontaneous emission from the active region of a semiconductor laser is completely determined by the spontaneous emission current and the concentration of charge carriers in the active region. Of course, the nonradiative recombination channel always exists, but modern epitaxial technologies make it possible to decrease it to a minimum, because of which the spontaneous luminescence quantum yield of lasers emitting at wavelengths of ~1 μm easily reaches values close to 100%. Therefore, if the spontaneous emission is measured under the conditions of completely suppressed stimulated emission (which was achieved in our experiment, Fig. 2), then it is possible to consider the existence of a dependence between the spontaneous luminescence intensity, the square root of the carrier concentration in the active region, and the pump current of the semiconductor laser.

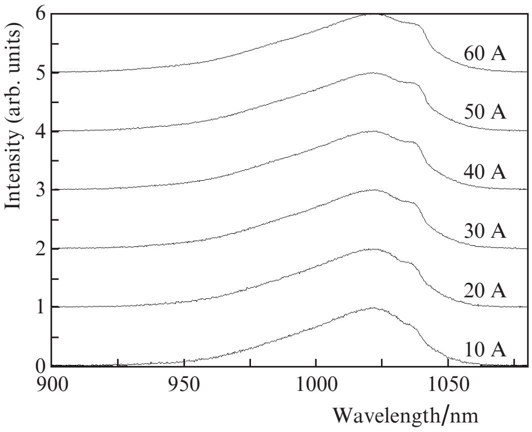

Figure 2. Spontaneous emission spectra of the laser in the pulsed regime at different pump current amplitudes. The long-wavelength part of the spectrum shows a line of scattered stimulated emission.

We studied a laser with a cavity of length 2600 μm and cleaved mirrors (reflection coefficients $R_1 = R_2 \approx 0.3$). The investigations were performed in two stages. At the first stage, owing to a changed geometry of the experiment, we measured the spontaneous emission spectra with almost complete absence of scattered stimulated emission line in the entire range of pump currents (Fig. 2). At the second stage, we recorded the amplitude of photoresponse pulses, which allowed us to plot the dependence of the relative increase in the spontaneous emission intensity on the pump current (Fig. 3). At a pump current of 60 A, the spontaneous emission intensity increased approximately by a factor of 1.35 with respect to the intensity at a current of 10 A.

Each threshold pump current density in the laser corresponds to a definite modal gain. The dependence of the modal gain on the threshold current density was experimentally

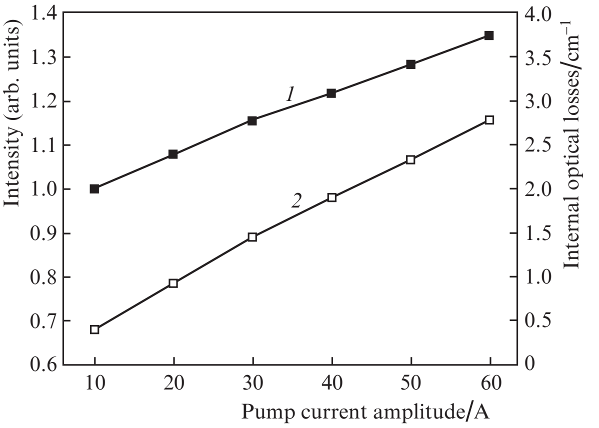

Figure 3. Relative increase in the spontaneous emission peak intensity (*1*) and corresponding calculated internal optical losses (*2*) as functions of the pump current amplitude.

determined as the sum of the internal and external optical losses for lasers with different cavity lengths made of one heterostructure (Fig. 4). The internal optical losses at the lasing threshold were determined by a standard method from the dependence of the inverse differential quantum efficiency on the cavity length for a series of semiconductor lasers [14]. In the studied laser structure, the internal optical loss near the lasing threshold $\alpha_{\rm in}$ was 0.4 cm^{-1} and identical for all lasers. The external optical loss was calculated for lasers with known cavity lengths and coefficients R_1 and R_2. In this case, an increase in the modal gain compensates an increase in the external optical loss with decreasing laser cavity length, which results in an increase in the threshold current density.

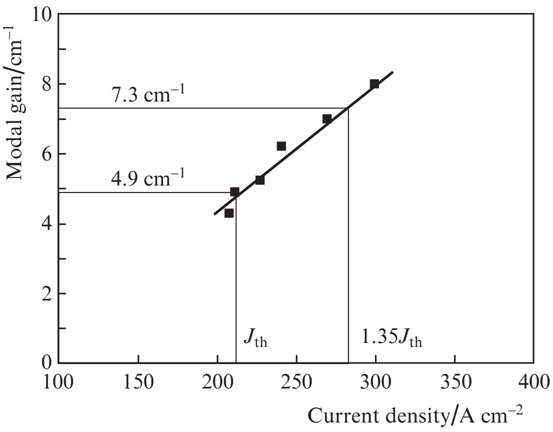

Figure 4. Modal gain vs. the threshold current density. Squares show experimental data, and the solid line corresponds to linear approximation.

In our case, the dependence shown in Fig. 4 makes it possible to determine the modal gain change with changing spontaneous emission current density in a laser with a fixed cavity length. The spontaneous emission intensity increases by a factor of 1.35 as the pump current increases to 60 A (see Fig. 3). Therefore, an increase in the spontaneous emission current density by a factor of 1.35 leads to an increase in the modal gain from 4.9 to 7.3 cm^{-1} (Fig. 4). Thus, the 1.35-fold increase in the spontaneous emission intensity increases the modal gain by 2.4 cm^{-1}. Since the increase in the modal gain is caused only by an increase in the internal optical losses $\alpha_{\rm in}$, we can conclude that these losses increase by 2.4 cm^{-1} and become equal to 2.8 cm^{-1} at a pump current of 60 A. Figure 3 presents the dependence of the internal optical losses on the pump current in a pulsed regime calculated by the above-described method.

4. Study of saturation of light–current characteristics of lasers in pulsed regime

The experimental light–current characteristic of the semiconductor laser studied above is shown in Fig. 5. We assume that the approximation $\eta_{\rm in} \approx 1$ (current leakage is small) is valid in the entire range of pulsed currents. Applying formula (1) with allowance for the above-described assumptions, we plotted the dependence of the internal optical loss on the pump current from the experimental light–current characteristic (Fig. 5). Comparing the obtained dependences of the internal optical loss on the pump current shown in Fig. 3 (calculated from the spontaneous emission intensity for a set of lasers with different lengths) and in Fig. 5 (calculated from the experimental light–current characteristic), we can ascertain that they almost completely coincide. This result shows that our assumptions on the smallness of current leakage and the weak dependence of the stimulated quantum efficiency on the pump current ($\eta_{\rm in} \approx 1$) are correct. In the opposite case, with decreasing stimulated internal quantum efficiency, the internal optical losses calculated from the experimental light–current dependence (Fig. 5) would be considerably lower than the losses calculated from the increase in the spontaneous emission intensity (Fig. 3). Thus, our experiments allow us to find the total internal optical losses in a laser structure at different pump currents. However, the experiments do not provide the possibility to estimate the change in the internal losses in individual heterolayers and directly determine the mechanisms responsible for the increase in these losses.

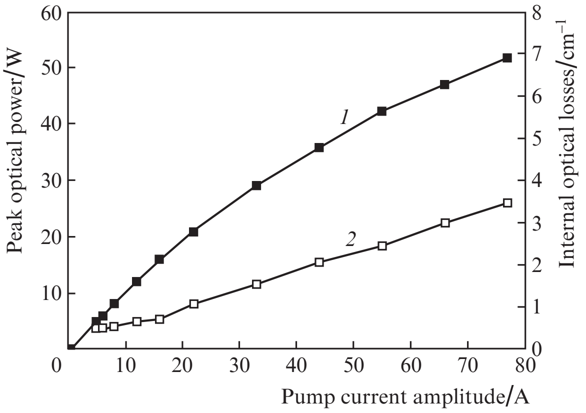

Figure 5. Peak optical power coupled out of the two cavity mirrors (*1*) and the calculated internal optical losses (*2*) as functions of the pump current amplitude.

5. Discussion of results and conclusions

(1) Using an original experimental method of studying semiconductor lasers at superhigh levels of pulsed current pump-

ing, we showed that an increase in the current amplitude leads to a proportional increase in the intensity of spontaneous emission from the active region.

(2) The dependence of the spontaneous emission intensity on the pump current allows one to calculate the corresponding dependence for the total internal optical losses for the studied lasers.

(3) The dependences of the internal optical losses on the pulsed pump current are calculated from the experimental light–current characteristic under the condition of small current leakage and a constant stimulated quantum efficiency ($\eta_{\text{in}} \approx 1$).

(4) The dependences of the total internal optical losses on the pulsed pump current in the semiconductor lasers determined by different methods have a quasi-linear character and well coincide at both low and superhigh pump currents.

The obtained agreement with the experimental data allows us to conclude that the increase in the internal optical losses is one of the reasons for the saturation of the light--current characteristic of the studied lasers with a broadened waveguide in the pulsed regime at superhigh pump currents. The physical mechanisms responsible for the increase in the internal optical losses with increasing pump current will be the subject of our future studies. It is very probable that one of these mechanisms is the non-instantaneous capture of charge carriers into the quantum-well active region [9], which can lead to a significant increase in the carrier concentration in the broadened waveguide of the laser at high pump currents.

Acknowledgements. This work was carried out according to the State Contract with the Ioffe Institute.

References

1. Brauch U., Loosen P., Opower H. *Topics Appl. Phys.*, **78**, 303 (2000).
2. Wang X., Crump P., Wenzel H., Liero A., Hoffmann T., Pietrzak A., Schultz C.M., Klehr A., Ginolas A., Einfeldt S., Bugge F., Erbert G., Tränkle G. *IEEE J. Quantum Electron.*, **46** (5), 658 (2010).
3. Vinokurov D.A., Kapitonov V.A., Lyutetskii A.V., Pikhtin N.A., Slipchenko S.O., Sokolova Z.N., Stankevich A.L., Khomylev M.A., Shamakhov V.V., Borshchev K.S., Arsent'ev I.N., Tarasov I.S. *Fiz. Tekhn. Polupr.*, **41** (8), 1003 (2007).
4. Slipchenko S.O., Sokolova Z.N., Pikhtin N.A., Borshchev K.S., Vinokurov D.A., Tarasov I.S. *Fiz. Tekhn. Polupr.*, **40** (8), 1017 (2006).
5. Miftakhutdinov D.R., Akimova I.V., Bogatov A.P., Gushchik T.I., Drakin A.E., D'yachkov N.V., Popovichev V.V., Nekrasov A.P. *Kvantovaya Elektron.*, **38** (11), 993 (2008) [*Quantum Electron.*, **38** (11), 993 (2008)].
6. Wenzel H., Crump P., Pietrzak A., Roder C., Wang X., Erbert G. *Opt. Quantum Electron.*, **41**, 645 (2010).
7. Ryvkin B.S., Avrutin E.A. *J. Appl. Phys.*, **97**, 123103 (2005).
8. Slipchenko S.O., Podoskin A.A., Shashkin I.S., Zolotarev V.V., Pikhtin N.A., Tarasov I.S. *Fiz. Tekhn. Polupr.*, **48** (5), 705 (2014).
9. Sokolova Z.N., Tarasov I.S., Asryan L.V. *Fiz. Tekhn. Polupr.*, **45** (11), 1553 (2011).
10. Bulaev P.V., Kapitonov V.A., Lyutetskii A.V., Marmalyuk A.A., Nikitin D.B., Nikolaev D.N., Padalitsa A.A., Pikhtin N.A., Bondarev A.D., Zalevskii I.D., Tarasov I.S. *Fiz. Tekhn. Polupr.*, **36** (9), 1144 (2002).
11. Shashkin I.S., Vinokurov D.A., Lyutetskii A.V., Nikolaev D.N., Pikhtin N.A., Rastegaeva M.G., Sokolova Z.N., Slipchenko S.O., Stankevich A.L., Shamakhov V.V., Veselov D.A., Bondarev A.D., Tarasov I.S. *Fiz. Tekhn. Polupr.*, **46** (9), 1230 (2012).
12. Shashkin I.S., Vinokurov D.A., Lyutetskii A.V., Nikolaev D.N., Pikhtin N.A., Rudova N.A., Sokolova Z.N., Slipchenko S.O., Stankevich A.L., Shamakhov V.V., Veselov D.A., Bakhvalov K.V., Tarasov I.S. *Fiz. Tekhn. Polupr.*, **46** (9), 1234 (2012).
13. Pikhtin N.A., Slipchenko S.O., Sokolova Z.N., Tarasov I.S. *Fiz. Tekhn. Polupr.*, **38** (3), 374 (2004).
14. Slipchenko S.O., Vinokurov D.A., Pikhtin N.A., Sokolova Z.N., Stankevich A.L., Tarasov I.S., Alferov Zh.I. *Fiz. Tekhn. Polupr.*, **38** (12), 1477 (2004).
15. Slipchenko S.O., Vinokurov D.A., Lyutetskii A.V., Pikhtin N.A., Stankevich A.L., Fetisova N.V., Bondarev A.D., Tarasov I.S. *Fiz. Tekhn. Polupr.*, **43** (10), 1409 (2009).
16. Slipchenko S.O., Podoskin A.A., Vinokurov D.A., Stankevich A.L., Leshko A.Yu., Pikhtin N.A., Zabrodskii V.V., Tarasov I.S. *Fiz. Tekhn. Polupr.*, **45** (10), 1431 (2011).
17. Slipchenko S.O., Shashkin I.S., Vavilova L.S., Vinokurov D.A., Lyutetskii A.V., Pikhtin N.A., Podoskin A.A., Stankevich A.L., Fetisova N.V., Tarasov I.S. *Fiz. Tekhn. Polupr.*, **44** (5), 688 (2010).